

Quality Assessment of Unmanned Aerial Vehicle
(UAV) Based Visual Inspection of Structures

by

G. Morgenthal and N. Hallermann

Reprinted from

Advances in Structural Engineering

Volume 17 No. 3 2014

Quality Assessment of Unmanned Aerial Vehicle (UAV) Based Visual Inspection of Structures

G. Morgenthal and N. Hallermann*

Institute of Structural Engineering, Bauhaus-Universität Weimar, Weimar, Germany

Abstract: This paper discusses the application of Unmanned Aerial Vehicles (UAV) for visual inspection and damage detection on civil structures. The quality of photos and videos taken by using such airborne vehicles is strongly influenced by numerous parameters such as lighting conditions, distance to the object and vehicle motion induced by environmental effects. Whilst such devices feature highly sophisticated sensors and control algorithms, specifically the effects of fluctuating wind speeds and directions affect the vehicle motion. The nature of vehicle movements during photo and video acquisition in turn affect the quality of the data and hence the degree to which damages can be identified. This paper discusses the properties of such flight systems, the factors influencing their movements and the resulting photo quality. Based on the processed data logged by the high precision sensors on the UAV the influences are studied and a method is shown by which the damage assessment quality may be quantified.

Key words: inspection, monitoring, UAV, image, blur, probability of detection.

1. INTRODUCTION

When focussing on the sustainability and resource-efficiency in the building and infrastructure sector, closer attention will in the future be paid to the reliability and serviceability of existing structures to extend their life time. This will require more sophisticated and effective methods for inspection and monitoring of structures, in order to assess their structural state and thus trigger repair and rehabilitation efforts. Particularly in relation to the safety requirements of critical infrastructures like bridges, towers, power plants or dams, the load bearing capacity is of high importance. An early identification of reduced capacity through deterioration and damage is a priority requirement.

Conventionally, the inspection of structures is based profoundly on visual investigation. Inspections of civil engineering structures are technically demanding and expensive, but particularly so where access to individual members is difficult. The inspection of critical structural components and spots which are hard to reach is mostly

done by large access units, scaffoldings or other specialised equipment. With the use of remotely controlled or semi-autonomously operating UAVs, the monitoring and inspection of buildings can be brought to a new level of quality and economy.

This paper summarises the typical properties of such small scale UAVs and studies the data acquisition in detail. It is based on the experience gained with two UAVs equipped with high definition photo and video equipment and tries to outline the opportunities that this technology may provide in the inspection of structures using some practical examples. Global positioning system (GPS) sensors and inertial measurement units (IMUs) built into the devices allow for advanced navigation and waypoint routing of the vehicles for inspection planning, live inspection and semi-autonomous flight missions. Data gathered can be geo-referenced for later storage in dedicated databases, such that inspection results can be related to locations on the structure and possibly be presented in 3D models, see (Wefelscheid *et al.* 2011).

*Corresponding author. Email address: norman.hallermann@uni-weimar.de.

A special emphasis of the paper is on studying the effects that influence the quality of the visual data. To this end, post flight data processing and data assessment is discussed. The wind stability of the UAVs is found to be a critical issue, which is studied in detail in relation to the achievable image quality and the effects this may have on automatic damage detection.

2. CONVENTIONAL INSPECTION OF LARGE STRUCTURES

Conventionally, inspections of large or hardly accessible structures like bridges, towers, dams or wind turbines or special parts of structures requires special equipment and specially trained staff. Figure 1 shows typical inspection units like elevating platforms, underbridge units or truck cranes. Inspection units are in most cases expensive custom products. Large trucks, special elevating platforms or scaffolding on buildings cause high logistical efforts and costs and also high personnel costs for the specially trained machine operators. These units can induce disturbances in using these structures (e.g. traffic jams). Specially trained staff, like industrial climbers, can get access to special parts of the structure but they can rarely evaluate what influences detected damages have on these structures. Therefore, they can only take Photos or Videos of the concerned part of the structure, which must be analysed by civil engineers.

3. UAV INSPECTION OF LARGE STRUCTURES

3.1. Types of UAVs

In general, unmanned aerial vehicles are aircrafts without human pilots. They can fly autonomously controlled by computers, be remotely controlled by a navigator/ pilot on the ground or semi-autonomously as a combination of both above mentioned capabilities. Initially, UAVs were developed for military operations during the 1970's and 1980's.

Recently however, a new generation of multirotor aircraft has emerged, that utilises fixed-pitch blades where control of the vehicle is achieved by differential rotor speeds. These small and very light (less than 5 kg) UAVs use brushless electrical motors and can be equipped with different kinds of high-end cameras. They are being used for different kinds of civil applications in the fields of photography, photogrammetry, geology, geography, agriculture, forestry, in environmental monitoring or for disaster management (Adams *et al.* 2012). A special application of such small UAVs in the field of civil engineering is discussed in this paper.

3.2. Principle Civil Applications and Limitations for Using UAVs

Today UAVs are ubiquitous in the tinker and hobby market. Further developed on these ideas, UAVs can be used professionally for different civil applications. Principally, UAVs are used for all kinds of airborne photo and video applications for advertising or in the real estate market for presentation. Public authorities find these small and flexible units useful for their applications. Security authorities and the police use UAVs for observation of unclear areas or mass events. Fire departments use these units for air based observation in critical fire situations (e.g. forest fires) to get an airborne overview of the fire area. Another field of application is the monitoring of vegetation and animals in agriculture or forestry (Israel 2012) and (Grenzdörffer 2013). In the field of heritage documentation, they are used for the documentation of historical areas and monuments. A further extensive application field of UAVs is the georeferenced photogrammetry, see (Everaerts 2008), (Zhang 2008) and (Eisenbeiß 2009). Among others, the use of UAVs in the field of civil engineering was investigated by (Derx *et al.* 2002), (Menti *et al.* 2007), (Eschmann *et al.* 2011) and (Kumar *et al.* 2013).



Figure 1. Conventional inspection units for large structures: elevating platform (left, Kaufer), underbridge unit (centre, WEMO-tec), truck crane (right, N.E. Bridge Contractors Inc.)

The use of small UAVs has many advantages in comparison to manned flight systems or other specific inspection units mentioned above. UAVs only need an operator on the ground for controlling the flight and the camera. They can be used in high risk situations without endangering human lives. Many flight systems are based on low cost technologies but they reach a high level of complexity for professional applications. Another advantage is the capability of fast real time data acquisition and the storage of all relevant flight data. Thus, they generate lower costs in comparison to large and personnel intensive inspection units. With intelligent features like GPS-control, UAVs are easy to handle for the pilot.

In spite of all these benefits, UAVs have some essential limitations, which confine the use of these systems. Due to the small payload, only small format and light digital compact cameras can be used for photo or video documentation. Furthermore, the limited payload allows only small battery packs, which causes a short flight time. Due to the low weight, the flight system is very sensitive to changes in the weather conditions, especially in critical wind situations. Unexpected flight situations or failures in the GPS-signal cause a change from the automatic flight mode into a manual mode, which requires a well-trained pilot to handle those critical situations. Currently, UAVs do not have an effective collision avoidance system. Other limits are given by the regulations of civil and security authorities. Often, a flight permission is required and autonomous flights are forbidden; there is a restriction for flights in line of sight.

3.3. Flight Systems

3.3.1. Standard specification

The flight systems used here are high-end professional systems, see Figure 2. They are based on a multirotor-platform with 8 rotors, which are arranged on two arms

mounted in V-shape configuration. The central unit with the camera is placed between both arms in the centroid of the system. This construction type is a patented product developed by the company Ascending Technologies.

The computing unit is primarily responsible for the flight control. Eleven different sensors (Accelerometer MEMSIC MXR9500G/M, Gyroscope ANALOG DEVICES ADXRS610, Compass HONEYWELL HMC5843), which send control signals to the computing unit at a high rate, are used to detect the position, orientation and to stabilise the flight system. Furthermore, all flight relevant data is logged by the computing unit. All data is stored on a standard SD-card and can be analysed after the flight.

The redundancy of each motor-rotor-combination, which allows a failure of up to 2 motors, guaranties a very high degree of safety. Other special safety features supports an easy handling. Equipped with an inertial measurement unit (IMU), a compass and a global positioning system-module (GPS) in combination with the GPS-position hold mode, which guarantees a continuously regulated flight, allows for stable flying in winds up to 12 m/s (6 bft).

With a standard payload of 500 g it is possible to install compact digital photo and video cameras of high quality on the flight unit. The cameras are installed on an actively compensated camera mount, which holds the camera continuously in a horizontally (roll stabilised) and vertically (pitch stabilised) stabilised positions. The special construction of the flight system and the modified camera mount allow a horizontal angular freedom of 360° and a camera tilting of 90° up and down. This affords a unique field of view. That is only possible with the flight systems of Ascending Technologies. The camera can be controlled and triggered remotely with the mobile ground station by the pilot of the flight unit or independently with a joystick by a second operator in complex flight situations. A live

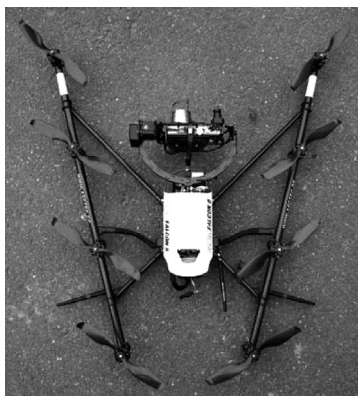


Figure 2. Flight system Falcon Photo with Panasonic Lumix TZ 22

stream of the camera to the display on the mobile ground station supports a certain controlling and orientation. The flight system, including the camera, is powered by an 8000 mAh battery pack, which allows for a flight time of approx. 16 – 20 minutes with the maximum payload.

3.3.2. Project related specifications

For the special application in the field of civil engineering, the manufacturing company created two enhanced flight systems for this research project. One flight system (Falcon Photo) used for photo and video data acquisition and the other one (Falcon Video) only used for HD-video data acquisition and live video stream analysis of damages. Both flight systems with the mobile ground station are shown in Figure 3.

The 150 g payload increased Falcon Photo can carry two types of digital photo cameras, a compact Panasonic Lumix TZ 22 with a high optical zoom factor and a Sony NEX 5 mirrorless DSLR interchangeable lens camera. Both digital cameras can also be used for HD-videos. The Falcon Video is equipped with an ultra-light HD BMS camera and a digital video link to get a live HD-video stream on a separate screen on the ground. The specifications are summarised in the following Table 1.

The pilot is supported by specific software features, which simplify the handling of the flight system. The “come home function” guarantees a safe landing when the connection between the ground station and the flight system is interrupted. The height control takes care that the flight system holds the altitude when the GPS-signal is too bad or interrupted. For a well-trained pilot, it is possible to steer the system only with the support of the barometric height control. The flight mission planning software allows pre-planned semi-autonomous GPS-controlled flights. During the flight, various flight system parameters are logged at 10 Hz frequency for a post-flight analysis. This also allows to reference all acquired data, including the photos, in time and position.

3.4. Examples of Application

The potential of using UAVs for the visual inspection of structures may be illustrated on various reference objects like chimneys, towers, bridges or historical buildings. Here the results with regard to achievable image quality of a typical scenario in civil engineering are shown on a natural stone structure. A 300 year old natural stone masonry tower of a church, shown in Figure 4 (left) was investigated using a UAV by performing an extensive photo and video data acquisition. A detailed post flight analysis of the building’s surface and a damage detection and localisation of defects like cracks or spillings on the masonry and the roof was performed.

The church is situated in the centre of a small village surrounded by other buildings very nearby. The tower is 44 m high and has a square section and a sectional slate roof dome and shows many damages and defects, especially at the roof and the joint between the masonry and the roof. The aim was to detect as much as possible damages or defects at a high degree of detail for the development of a reliable rehabilitation concept. Due to the high quality equipment and a well trained pilot, which allows a flight in very close proximity to the structure, it was possible to detect even very small damages, e.g. very thin cracks between several bricks. Figure 4 (right) shows some detected damages at the masonry and the slate roofing in detail.

To get a more intensive idea of the potential of the flight system and achievable image quality the following Figure 5 shows an exemplary selection of images and damage patterns on different structures over increasing heights up to 225 m. The left figure shows detected cracks at a wall roof joint on an old hangar in a height of 15 m in an distance to the structure less than 5 m. The middle one shows the machine house of a wind turbine with rusty spots in a height of 100 m taken from a distance of 10 m. The right figure shows the top of a chimney and the inner brick lining with some missing



Figure 3. Flight systems with mobile ground station (remote control): Falcon Photo (left), Falcon Video (right)

Table 1. Specifications of flight systems

Falcon – Photo system	Falcon – Video system
<ul style="list-style-type: none"> - Payload increased flight system (+ 150 g) - Digital camera 1 <ul style="list-style-type: none"> Type Panasonic Lumix DMC TZ 22 14.1 megapixel 16 × optical zooming Focal length 24 – 384 mm (Leica DC wide angle lens) Full-HD-Video (1080/50 p) - Digital camera 2 <ul style="list-style-type: none"> Type Sony NEX 5 14.2 megapixel APS-C sensor Prime lenses (interchangeable) Wide angle lens 16 mm Normal lens 30 mm Normal to short tele focus lens 50 mm Full-HD-Video (1080/50 p) 	<ul style="list-style-type: none"> - BMS Digital Video link 5.8 GHz for live video stream (HD-Quality) - Video camera <ul style="list-style-type: none"> BMS Ultra Light HD camera Full-HD-Video 10 × optical zoom



Figure 4. Masonry church 44 m (left), detected slate roofing damages (top right, elevation $h = 40$ m, object distance $L \approx 10$ m), detected critical cracks at masonry corner roof joint (bottom right, $h = 25$ m, $L \approx 5$ m)

bricks at a height of 225 m taken from a distance of 25 m from the chimney.

As can be seen, under good conditions very detailed image data can be generated of structural details that are

otherwise very difficult to access. However, the influence of environmental effects may affect the image quality, which shall be studied in more detail subsequently.



Figure 5. Examples for possible image quality: cracks in a wall roof joint (left, $h = 15$ m, $L < 5$ m), rusty spots on wind turbine machine house (centre, $h = 100$ m, $L \approx 10$ m), damages on inner brick lining of a chimney (right, $h = 225$ m, $L \approx 25$ m)

4. VEHICLE MOTION

4.1. Motion Effects Influencing Image Quality

The quality of an image is typically characterised by several image parameters, so called subjective image quality assessment (IQA) metrics like sharpness, noise, contrast (dynamic range) and colour fidelity. An efficient and robust IQA free of subjective influences requires objective IQA metrics. Conventional objective IQA methods are based on a “distortion free” reference image and use e.g. intensity correlating Mean Square Error (MSE), Peak Signal to Noise Ratio (PSNR) or Normalised Cross-Correlation (NCC) for the quantification of image quality, see more in (Chandler 2012) and (George *et al.* 2013).

Technically, the image quality is affected by the technology used, i.e. optics including focusing accuracy, digital photo sensor properties and in-camera image processing, as well as the environmental conditions like lighting, haze etc. and the properties of the object (contrast, surface reflectivity etc.). In the context of using UAVs as a platform, the most prominent effect is the motion blur, which leads to reduced image sharpness. Movements of the camera during exposure result in a blurred image that provides less detail and makes identifying features more difficult. Therefore, the vehicle movements are of specific interest and shall be focused on here.

4.2. Wind Effects

The control and navigation algorithms of modern UAV are highly advanced, particularly on professional grade flight systems. Numerous high resolution sensors monitor the vehicle position and motion, using Global Positioning Systems as well as Inertial Measurement Units and powerful signal processing hardware. The algorithm corrects environmental effects to stabilise the flight systems, minimizing motion during photo recording. Whilst constant wind speeds can be reliably corrected for, fluctuations in wind speed and direction lead to time-varying aerodynamic forces on the vehicle,

which need to be corrected, resulting in vehicle motion due to the correction lag. It is hence these wind changes that are of major importance in studying vehicle motion and image quality.

Fluctuations in wind speed and direction may be due to two effects: atmospheric turbulence and body-generated turbulence. Atmospheric turbulence is always present, resulting from the nature of the atmospheric boundary layer influenced by the surface roughness of the earth. This turbulence, which is commonly expressed by the Turbulence Intensity, increases towards the ground and is highest in areas of strong surface roughness such as built-up environment, hilly terrain or significant vegetation. One may thus expect stronger fluctuations when operating in cities and close to the ground.

When operating UAVs near structures, the fluctuations generated by the local aerodynamics around the structure may also be of significance. Even in uniform wind flow typically non-streamlined structural geometries will generate turbulent flow features due to boundary layer flow separation and the resulting vortical flow features convected downstream. These processes of vortex shedding and wake creation are well understood as a result of many studies in the field of Bluff Body Aerodynamics (Morgenthal 2002) and (Morgenthal 2005). In the context of using UAVs to document features of large structures, the body-generated turbulence deserves a closer look.

Some key aspects may be identified by looking at a vertical structure like a tower or a chimney. Figure 6 shows a twin tower arrangement that has been studied by a two-dimensional Computational Fluid Dynamics simulation (Morgenthal and Walther 2007). The figure shows a time-averaged velocity magnitude field, from which the shielding and accelerating regions of the flow can be identified. Some areas show flow speeds of significantly less than the free stream wind speed U_∞ , whilst in some areas speeds of as much as 60% higher than free stream speeds are present. When moving the

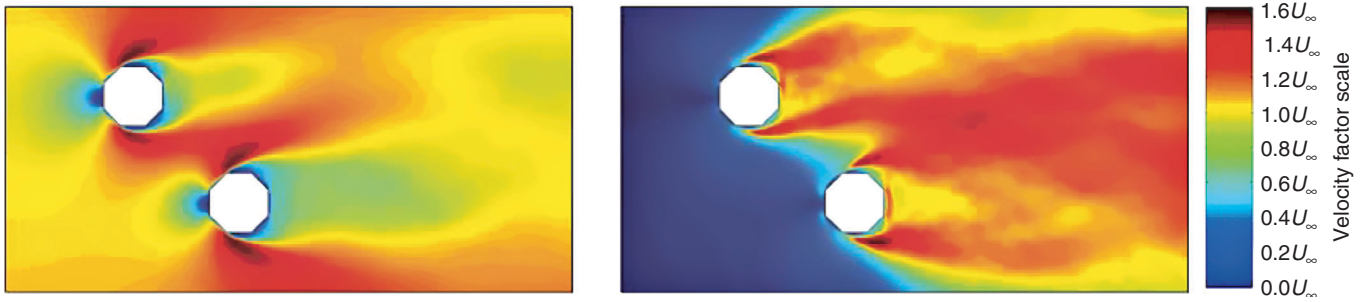


Figure 6. CFD simulation of octagonal twin tower, wind from left side under 45°: average flow velocity magnitude (left) and standard deviation (right)

UAV from a low speed to a high speed region and vice versa, the system will exhibit significant control motion (e.g. overshooting) due to the strong velocity gradients to be corrected for. Also shown in the figure are the fluctuations of the flow, expressed by the standard deviation of flow speed over time. The strong fluctuations are identified in the region of separated flow behind the section assembly. The UAV, if held at a position, experiences strong flow fluctuations and will constantly move due to the corrections required.

The example shown only highlights the main phenomena, every structure under a certain direction of wind speed will exhibit its own flow characteristics. Whilst these effects may be predicted by simulations or wind tunnel tests, they cannot be reduced and the impact on the vehicle will inevitably affect image quality. It is hence of interest, what magnitude of vehicle motion will result from certain degrees of turbulence intensity.

4.3. Monitoring Vehicle Motion and Image Frame

The time-dependent motion of a UAV under the influence of atmospheric turbulence has been studied to quantify the effect of wind speed fluctuations on the flight control system. To this extent, the accelerations,

angular rotations and elevation data logged by the flight system were analysed. The results that the vehicle movements will have on the quality of recorded images are shown later in this paper.

To analyse the effect of UAV motion on the photo taken by the camera, a coordinate system relating flight system and photo frame has been introduced, see Figure 7. Here, x , y and z describe the movement of the flight system in horizontal and vertical direction (right/ left, forward/ backward, up/ down respectively). The angle φ_z describes the rotation about the vertical axis, called yaw. The angles φ_y and φ_x describe the rotation about the horizontal axes, called roll and pitch respectively.

Assuming that the camera is rigidly fixed to the flight system (no active stabilization) and a constant distance L to the considered planar area, the produced displacements on the photo frame can be calculated by the relative translational and rotational changes in the movement of the flight system. The translational changes in horizontal and vertical direction cause equal displacements (x' and z') in the photo frame. The rotations cause additional linear displacements on the photo frame while the roll creates no displacement of the center point of the photo frame. Thus, the largest

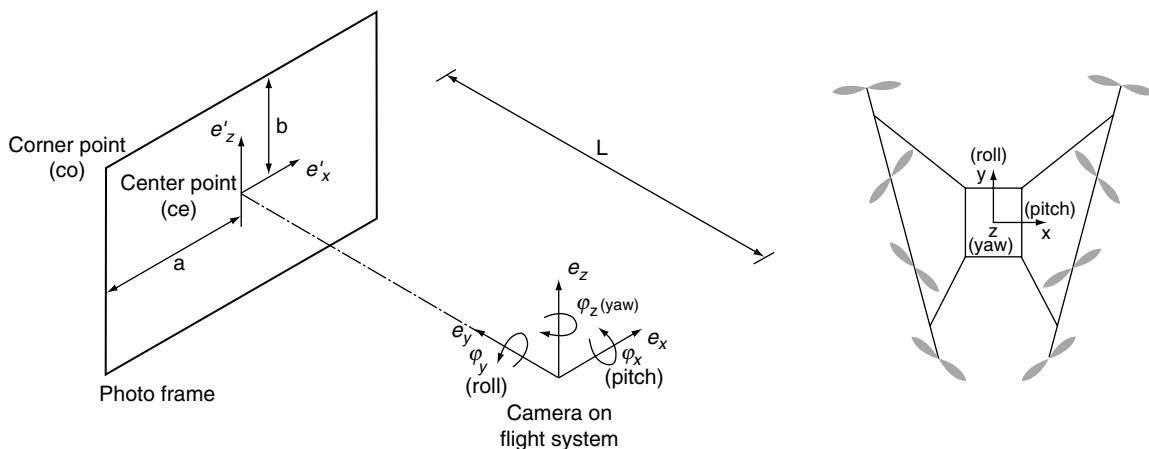


Figure 7. Definition of coordinate system of photo frame and flight system

displacements occur in the corner point (co) of the photo frame, which will be considered further. The displacements of the corner point of photo frame are shown in Figure 8. Based on the assumption of small changes in the angle they can be calculated by

$$x'_{co} = (x + L \cdot \varphi_z - b \cdot \varphi_y) \quad (1)$$

$$z'_{co} = (z - L \cdot \varphi_x - a \cdot \varphi_y) \quad (2)$$

4.4. Test Mission Setup

Using the relationships introduced above, an experimental program was developed to study the relationship between the wind conditions and the vehicle motion. Namely, the flight system was operated

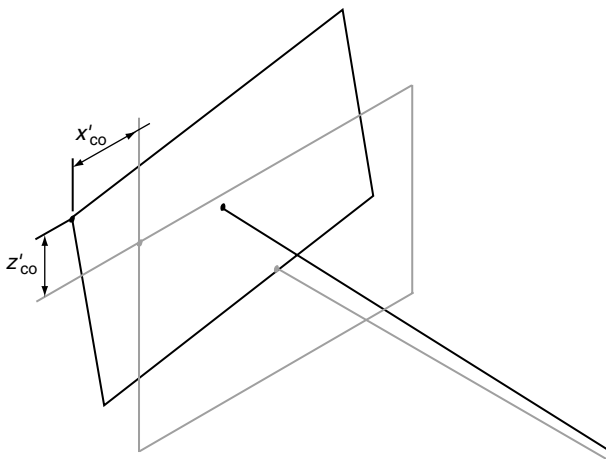


Figure 8. Displacements of photo frame corner point

at different altitudes and the vehicle motion quantified in relation to the height. An autonomous flight mission was set up to minimise user influence. Figure 9 shows the test mission setup, where steps of 20 m from 20 m up to 140 m elevation were held over constant periods of 90 seconds at a constant yaw (0° towards north) over the whole flight. The position and orientation of the flight system is controlled by the internal sensor-based control system. The altitude is controlled by the barometric height, the accuracy of which is higher than the GPS height control for short periods of time. This was tested by the manufacturing company of the UAVs in laboratory and practical tests. In spite of the barometric height control mode, the flight system moves continuously up and down caused by wind and the inaccuracy of the barometric height sensor (Freescale semiconductor MPX-series), which has a maximum accuracy range of 2 m. However, the flight tests show that in most cases the accuracy is better than 2 m, nearly in a range of 1 m, which is acceptable for most applications of these flight systems. Figure 9 also shows a sample extracted time window of 60 seconds at a height of 80 m. It is this time window that shall be analysed in greater detail in the next section. The majority of the altitude variations are attributed to a time dependent drift of the sensor data of the barometric height sensor rather than actual vehicle vertical motion, which is important for post-processing of the flight path.

4.5. Test Mission Results

The translational and rotational components of the vehicle displacements were calculated from the accelerations and angular rotations logged by the flight system at 10 Hz. By integrating the accelerations once and twice, the velocities and displacements can be

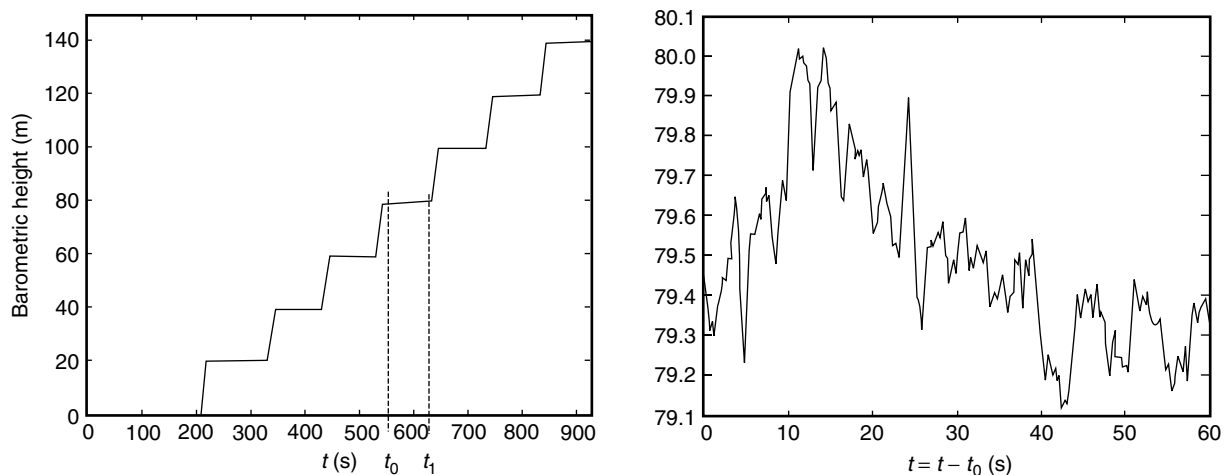


Figure 9. Barometric height record of flight path: total test mission (left), extraction t_0 to t_1 (right)

determined respectively, by

$$a_x = \ddot{x} = \frac{d^2x}{dt^2} \text{ and } a_z = \ddot{z} = \frac{d^2z}{dt^2} \quad (3)$$

$$v_x = \dot{x} = \int_0^t \ddot{x} dt \text{ and } v_z = \dot{z} = \int_0^t \ddot{z} dt \quad (4)$$

$$x = \int_0^t \dot{x} dt \text{ and } z = \int_0^t \dot{z} dt. \quad (5)$$

Figure 10 and Figure 11 show the time histories for the logged accelerations and the resultant velocities and displacements for the considered time window in x- and z-directions. The diagram shows the unfiltered acceleration data plotted from the logfiles of the flight system. When integrating, significant drift is seen in velocities and displacements, as identified by the thin line in the particular diagram. This drift was corrected by a Butterworth high pass filter used on the accelerations. Additionally, a reference line representing the barometric height is provided for the z-direction.

The above calculated translational displacements in

the x- and z-direction and the displacements caused by the rotations can be combined into a displacement path for the virtual observed corner point. Figure 12 shows the resultant displacement path of the corner point of the photo frame over the extracted time window. Herein, the total envelope of vertical movements of approximately 1 m and horizontal movements of 2.25 m illustrate the wind sensitivity of the flight system. In most of the test cases the movements in the vertical direction are less than the movements in the horizontal direction, which is a result of vertical turbulence component as well as flight system characteristics.

To provide a better insight into the nature of the displacement path, two separate displacement contributions to the corner point displacements of the photo frame are shown in Figure 13. The left diagram illustrates the displacements of the observed point caused by vehicle translation (x and z) only, being essentially the movement of the flight system itself. The right diagram shows the point displacements arising from vehicle rotations. As is apparent, the influence of the pitch, roll and yaw rotations of the flight system induce only a relatively small component of the total image frame displacements. Since only pitch and roll vehicle motion can be compensated by a stabilised camera mount, this allows to conclude that camera stabilization is of little

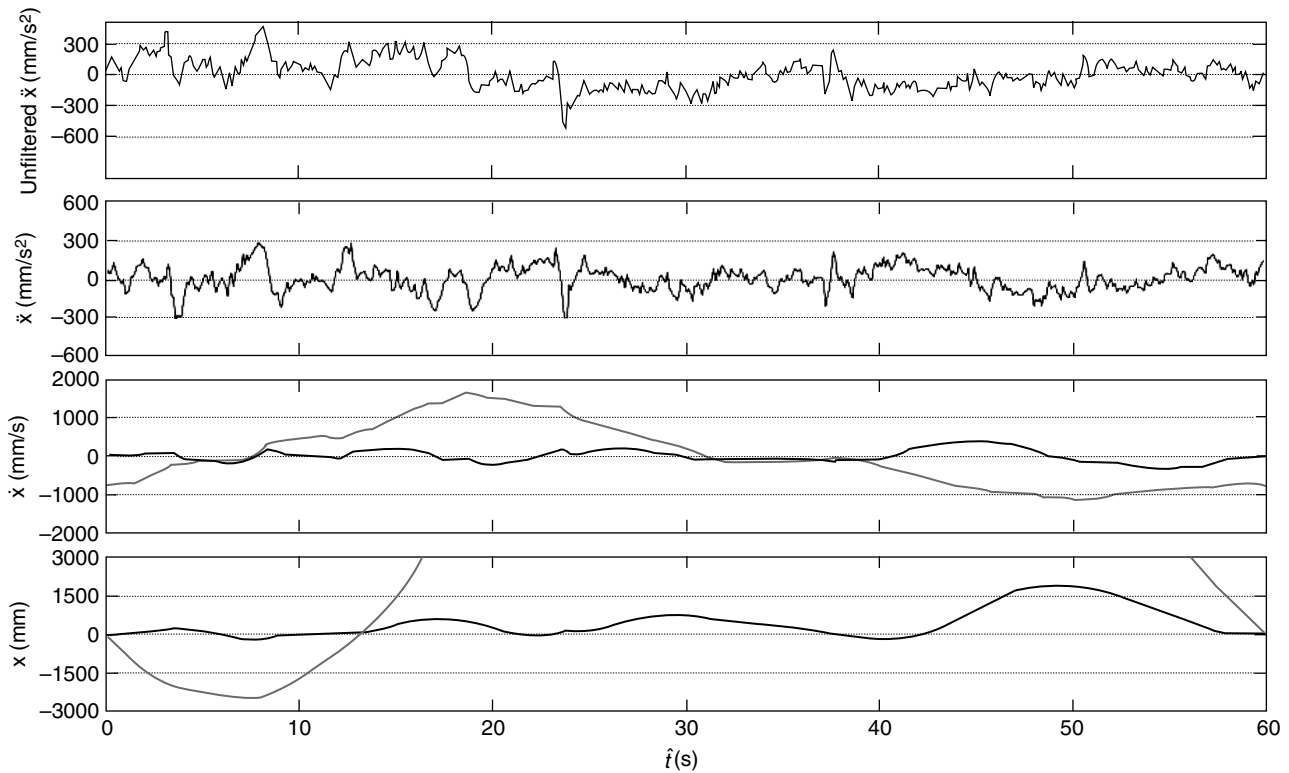


Figure 10. Time history (from top to bottom): unfiltered accelerations, filtered accelerations, velocities and displacements of the flight system in x-direction; (—) unfiltered and (—) filtered signal

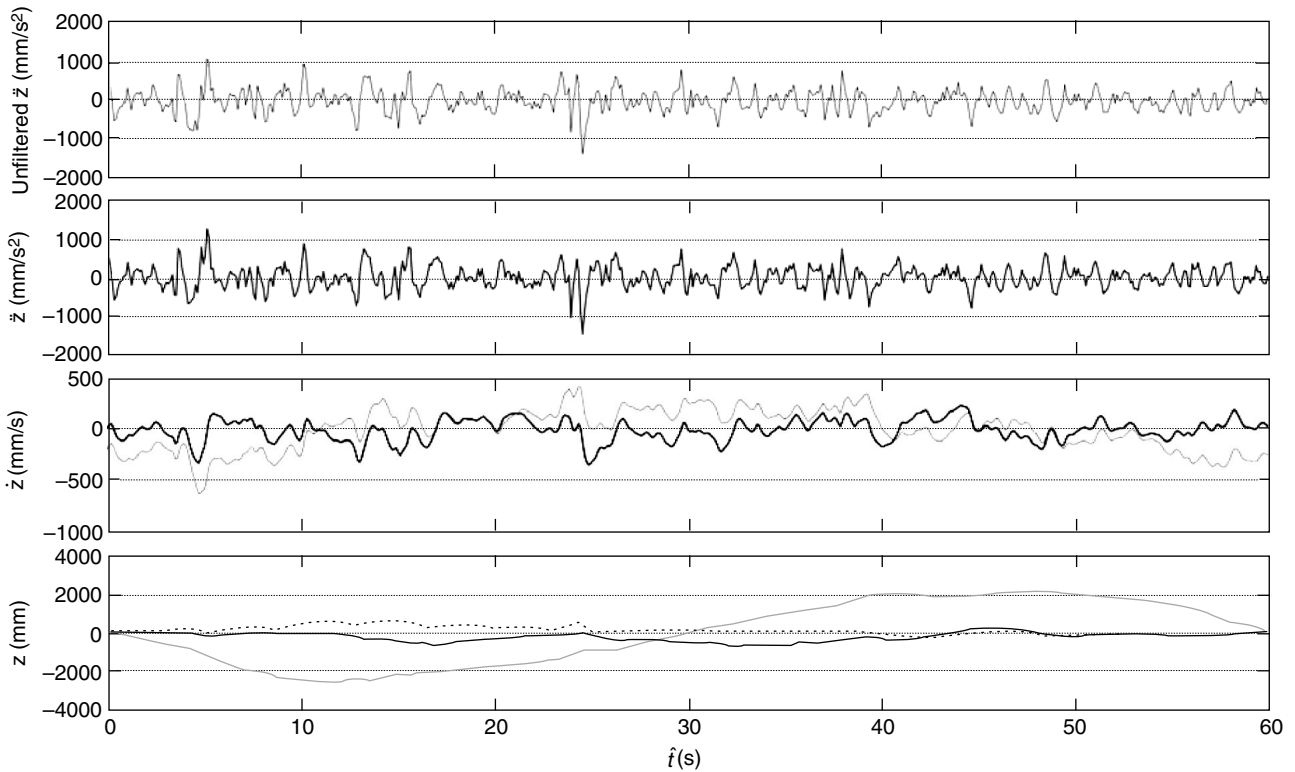


Figure 11. Time history (from top to bottom): unfiltered accelerations, filtered accelerations, velocities and displacements of the flight system in z-direction; (—) unfiltered, (---) filtered signal and (· · ·) barometric height

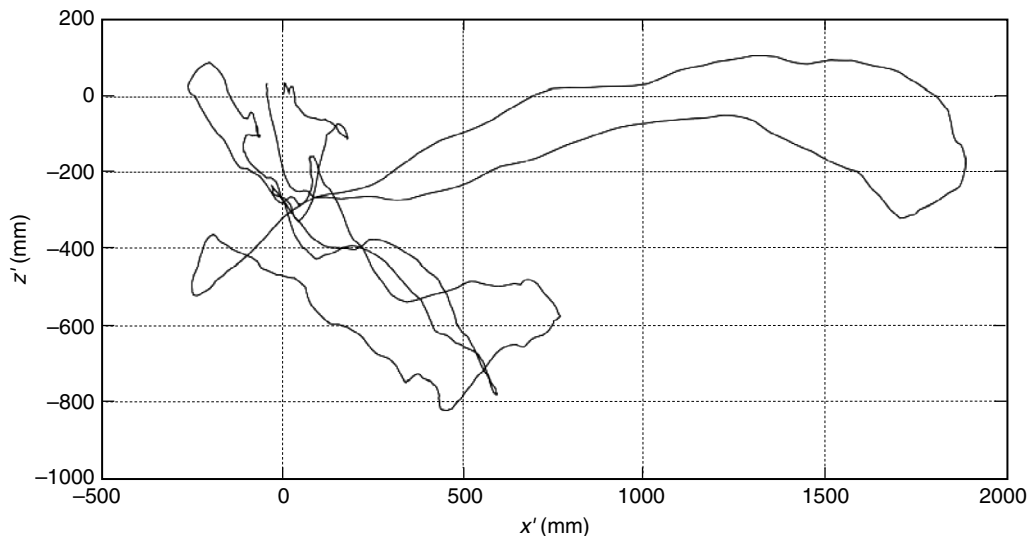


Figure 12. Displacement path of photo frame corner point for the 60 s time sample

help in such UAV subjected to natural wind.

4.6. Statistical Analysis of Frame Displacements

In the next step, the vehicle motion is analysed statistically. The vehicle velocity is studied, as this is directly related to image blur during image exposure.

The blur displacement would be image frame velocity multiplied by shutter speed (exposure time). The velocity magnitude of the corner point can be calculated as

$$v_{co,abs} = \sqrt{\dot{x}'_{co}{}^2 + \dot{z}'_{co}{}^2} \quad (6)$$

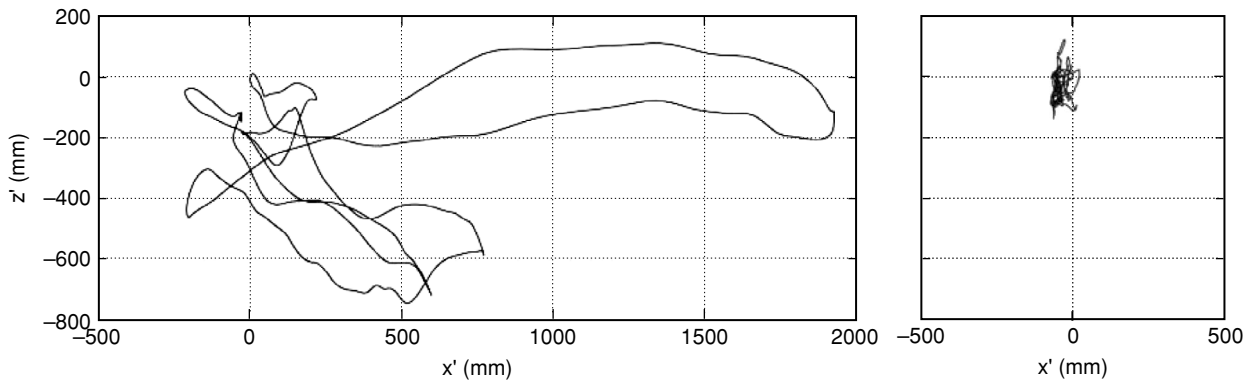


Figure 13. Contributions to corner point displacements: due to translation (left), rotation (right)

The velocity magnitude time histories are converted into histograms by sorting the data into bins. Then the probability distributions are created by the cumulative summation over the histogram data. Figure 14 shows the normalised cumulative summation of the velocity magnitudes for the 60 s sample time windows (left) and for all 90 s time windows at different heights (right). The influence of elevation is clearly seen. The adverse effect of the wind reduces with height, which is due to the characteristics of the atmospheric boundary layer, where turbulence is largest near the ground. One outlier is identified; otherwise the tendency is very well captured and could be related to turbulence intensities in a future experiment where wind data are studied in detail.

5. EFFECT OF VEHICLE MOTION ON IMAGE QUALITY

5.1. Motion Blur Simulations

Here, the effect that the continuous movement of the UAV-mounted camera has on the image quality shall be

studied by a motion blur simulation. To this end, a real photo of a wall with a cracked plaster surface is used. The effects of frame displacement can be simulated by a linear motion blur filter applied to the image. Here, the shift can be directly related to the movement of the flight system during the shutter speed t_s . The shift d_{mb} can be calculated by

$$d_{mb} = v_{co,abs} \cdot t_s \tag{7}$$

The corner point velocity is applied to the entire image, which is on the safe side with regard to estimating the adverse effect of movement. As was shown above, the camera rotation is of minor importance, such that however the corner does not more significantly more than the centre region of the image, thus making this a good approximation.

To simulate the motion blur effect on the airborne photos a ground based photo was taken by a Sony NEX 5N with a resolution of approximately 16 mega pixels,

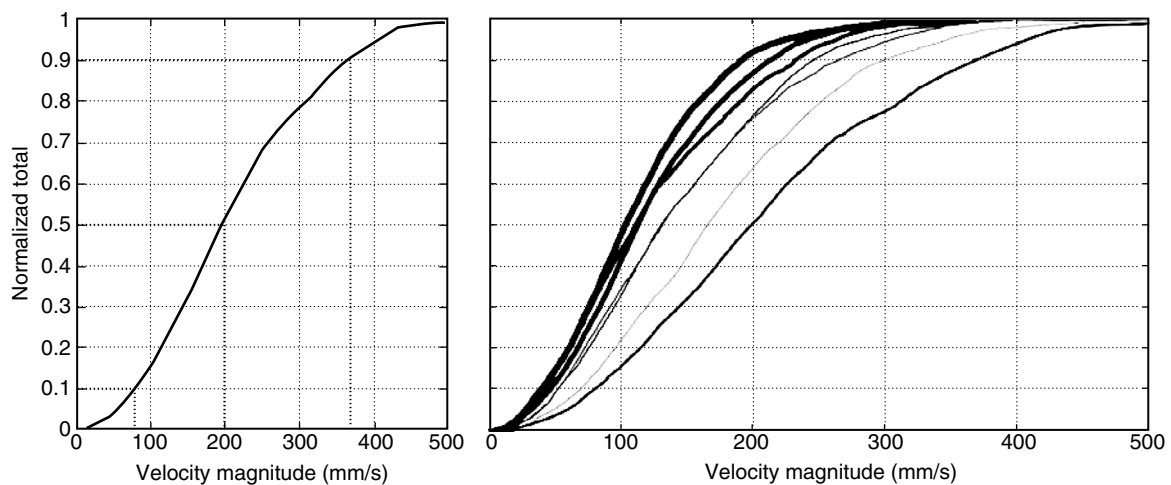


Figure 14. Cumulative summation of velocity magnitude: extraction in 80 m (left), all heights (right) heights are described by increasing thickness of the lines, thinnest line for the height of 20 m, thickest for 140 m

similar to the camera on the flight system. With the referenced data of the dimension of the CMOS APS-C sensor, the focal length of the camera and the distance L to the object, it is possible to determine the physical dimensions of the photo. The photo simulation was generated for a centred image section of the original photo shown in Figure 15. The geometrical relationship between the observed frame dimension a_f and b_f at a distance L from the camera and the sensor dimension a_s and b_s for a given focal length f can be expressed as

$$\frac{a_f}{L} = \frac{a_s}{f} \quad \text{and} \quad \frac{b_f}{L} = \frac{b_s}{f}, \quad (8)$$

see Figure 15.

The image properties and the photo parameters of the image section considered are summarised in the following Table 2. Figure 16 demonstrates the simulation of the motion blur for the 10th, 50th and 90th percentile of the velocity magnitude, using the cumulative distribution function from the flight at 80 m altitude discussed above. The particular velocities and the calculated shifts are assigned to the considered percentile. It is clear to see that the image quality decreases by the increasing velocity.

5.2. Effect of Motion Blur on Damage Detection using Computer Vision Methods

Motion blur effectively reduces the fidelity, i.e. quality of the image. This poses the question as to a sensible definition of image quality in the context of damage detection on structures. Identification of a damage pattern will be a subjective issue if performed by a human being. In the future it will however be of interest to perform automated damage recognition using Computer Vision methods. This also allows to rationalise the quality assessment of damage detection.

Here, the aim is not to perform practically relevant damage detection or to find optimised Computer Vision methods, but rather to outline a principal approach to assessing detection quality. Of particular interest in the assessment of major structures may be the identification of cracks in concrete surfaces. Figure 17 shows an example of a self-developed Computer Vision pattern recognition algorithm applied to the photo of such a crack. The left side shows the original crack and a very good result of the crack detection. The right side shows an image with a reduced image sharpness due to motion blur and the effect on the crack detection. The motion blur results in a reduced accuracy of crack detection when using the same

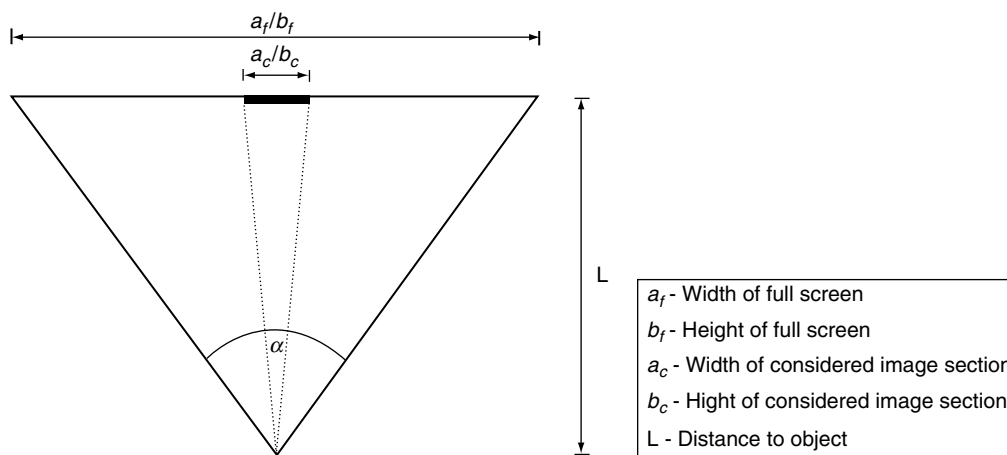


Figure 15. Dimension of the considered image section of the original photo

Table 2. Image properties and photo parameters

APS-C sensor	$\alpha = 23.4 \text{ mm} = 4912 \text{ pixels}$ $b = 15.6 \text{ mm} = 3264 \text{ pixels}$	210 pixels/mm
Original photo	$a_f = 2925 \text{ mm} = 4912 \text{ pixels}$ $b_f = 1950 \text{ mm} = 3264 \text{ pixels}$	1.68 pixels/mm
Considered image section	$a_c = 368 \text{ mm} = 618 \text{ pixels}$ $b_c = 696 \text{ mm} = 1165 \text{ pixels}$	1.68 pixels/mm
Distance to object	$L = 2000 \text{ mm}$	
Focal length	$f = 16 \text{ mm}$	
Shutter speed	$t_s = 1/80 \text{ s}$	

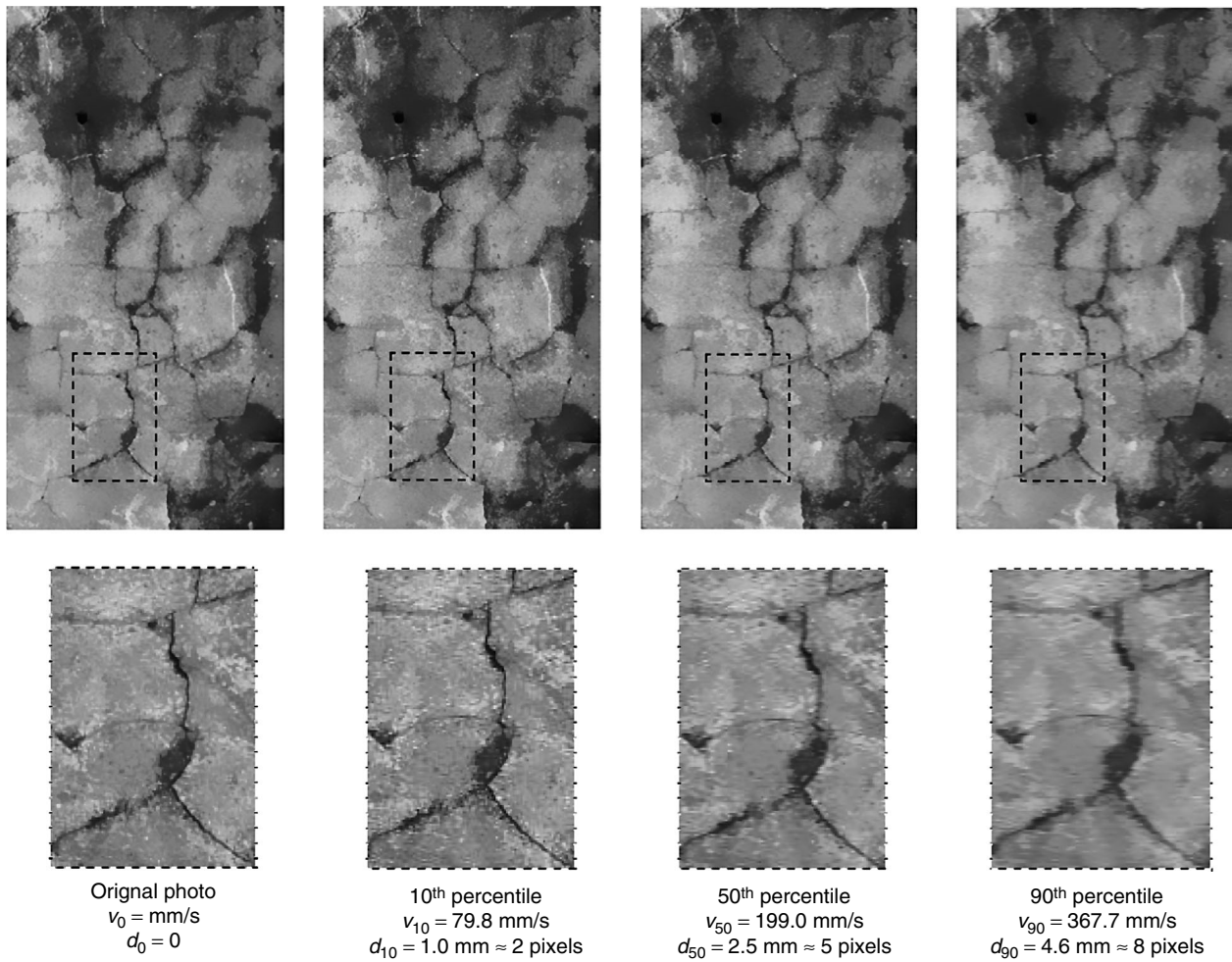


Figure 16. Motion blur photo simulation of image section

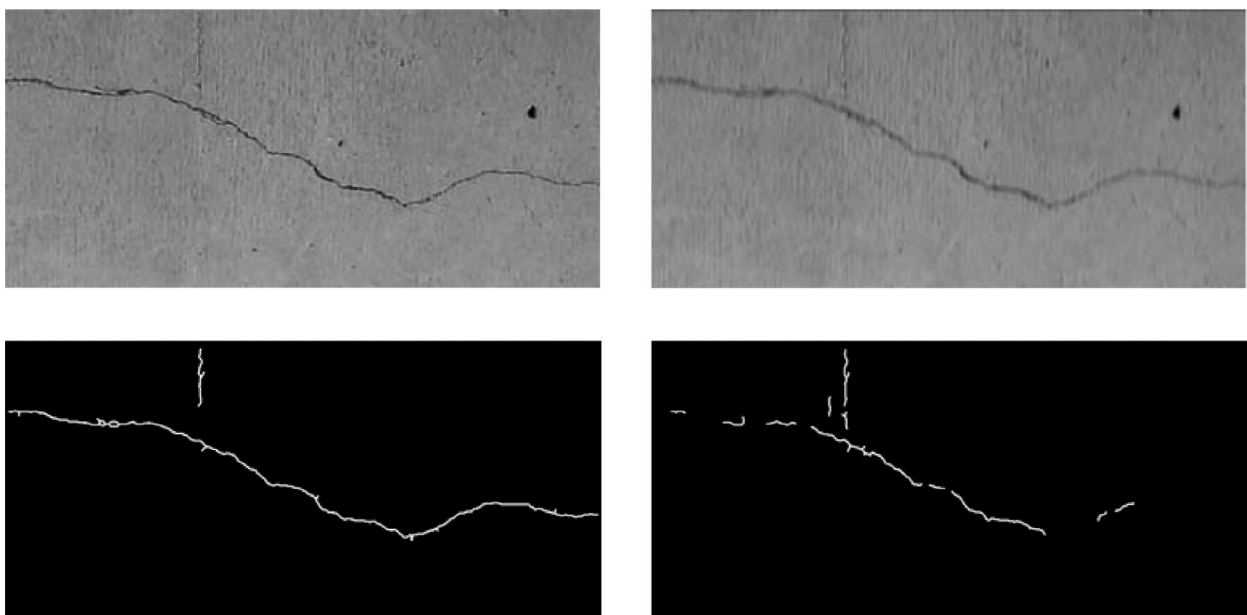


Figure 17. Automatic crack detection: original photo of crack in a concrete member (top left) with CV-based crack detection (bottom left), corresponding results of blurred photo (right)

algorithm. By quantifying the amount of the actual damage that is identified, it would be possible to quantify a detection quality. This quality could then be related back to the different parameters influencing the image quality, e.g. wind parameters, structural aerodynamics, UAV properties etc. to determine a probability of detection (POD) for certain flight conditions. By doing this, the automatic damage identification could be rationalised and the achievable detection accuracy assessed. This will be the subject of future work by the authors.

6. SUMMARY, CONCLUSIONS AND OUTLOOK

This paper outlined the possible applications of UAV to generate detailed images of structural details to support the condition assessment of civil structures. The potential for such applications is enormous, particularly where access is difficult these airborne vehicles can reduce costs and generate image data very efficiently. However, the flight systems are subject to environmental effects and a major contributor affecting image quality is the continuous movement of the vehicle due to fluctuations in wind speed and direction. The paper shows methods to assess these influences and to trace the effects all the way to be the automatic detection of damages using Computer Vision methods. Applying this methodological framework it would be possible to compute a probability of detecting certain damage patterns for a given set of environmental conditions. Such analyses would pave the way to a quantified and thus rationalised quality assessment of UAV-based structural condition assessment, thus further enhancing the potential use of this technology.

ACKNOWLEDGMENTS

The authors gratefully acknowledge the contributions by Peter Olney and the technical support by Ascending Technologies. Furthermore, special thanks go to Prof. Dr.-Ing. Volker Rodehorst (Chair of Computer Vision in Engineering, Bauhaus-Universität Weimar) and Eugen Müller for providing the Computer Vision algorithm.

REFERENCES

- Adams, S., Levitan, M. and Friedland, C. (2012). "High resolution imagery collection utilizing unmanned aerial vehicles (UAVs) for post-disaster studies", *ATC & SEI Conference on Advances in Hurricane Engineering: Learning from Our Past*, Miami, Florida, USA, pp. 777–793.
- Ascending Technologies (2013). URL: <http://www.asctec.de>.
- Chandler, D.M. (2012). "Seven challenges in image quality assessment: past, present, and future research", *ISRN Signal Processing*, Vol. 2013.
- Derx, F., Dumoulin, J., Sorin, J.L. and Legeay, V. (2002). *Concept de Plate-Forme Mobile Instrumentée (PMI) pour l'inspection des Ouvrages d'art*, Laboratoire Central des Ponts et Chaussées, Paris, France.
- Eisenbeiß, H. (2009). *UAV Photogrammetry*, PhD Thesis, ETH Zurich, Switzerland.
- Eschmann, C., Kuo, C.M., Kuo, C.H. and Boller, C. (2012). "Unmanned aircraft systems for remote building inspection and monitoring", *6th European Workshop on Structural Health Monitoring*, Dresden, Germany.
- Everaerts, J. (2008). "The use of unmanned aerial vehicles (UAVs) for remote sensing and mapping", *XXI ISPRS Congress*, Beijing, China.
- George, A.G. and Kethsy Prabavathy, A. (2013). "A survey on different approaches used in image quality assessment", *International Journal of Emerging Technology and Advanced Engineering*, Vol. 3, No. 2, pp. 35–41.
- Grenzdörffer, G.J. (2013). "UAS-based automatic bird count of a common gull colony", *UAV-g 2013*, Rostock, Germany.
- Israel, M. (2011). "A UAV-based roe deer fawn detection system", *Conference on Unmanned Aerial Vehicle in Geomatics*, Zurich, Switzerland.
- Kaufer (2012). URL: <http://www.kaufer.es>. (accessed on 27/07/2012)
- Kumar, S.K., Rasheed, A.M., Kumar, R.K., Giridharan, M. and Ganesh. (2013). "Dhaksha, the unmanned Aircraft System in its new avatar automated aerial inspection of India's tallest tower", *UAV-g 2013*, Rostock, Germany.
- Menti, N. and Hamel, T. (2007). "A UAV for bridge inspection: visual servoing control law with orientation limits", *Automation in Construction*, Vol. 17, No. 1, pp. 3–10.
- Morgenthal, G. (2002). *Aerodynamic Analysis of Structures Using High-resolution Vortex Particle Methods*, PhD Thesis, University of Cambridge, UK.
- Morgenthal, G. (2005). "Advances in numerical bridge aerodynamics and recent applications", *Structural Engineering International*, Vol. 15, No. 2, pp. 95–100.
- Morgenthal, G. and Walther, J.H. (2007). "An immersed interface method for the vortex-in-cell algorithm", *Computers and Structures*, Vol. 85, No. 11-14, pp. 712–726.
- N.E. Bridge Contractors Inc. (2012). URL: <http://www.bridgeriggers.com>. (accessed on 27/07/2012).
- Wefelscheid, C., Hänsch, R. and Hellwich, O. (2011). "Three-dimensional building reconstruction using images obtained by unmanned aerial vehicles", *Conference on Unmanned Aerial Vehicle in Geomatics*, Zurich, Switzerland.
- WEMO-Tec GmbH (2012). URL: <http://www.wemo-tec.com>. (accessed on 27/07/2012).
- Zhang, Y.J. (2008). "Photogrammetric processing of low altitude image sequences by unmanned airship", *XXI ISPRS Congress*, Beijing, China.